shape. Only loads not sensitive to applied voltage can be driven efficiently. Second, magnetic storage gives output pulses with impedance lower than that of most sources. Finally, the opening switch is usually destroyed. For a detailed description of opening switch technology, see Guenther et al.[5]

The widely developed opening switches are:

- *Exploding foil or wires*, frequently of copper, immersed in an insulating gas or liquid, open the circuit. They are designed to have high rates of increasing resistance, leading them to vaporize at peak current. Examples of their use are shown below.
- *Plasma erosion opening switch* (PEOS) can in principle be operated repetitively. In the plasma erosion switch, a plasma injected into a vacuum gap between the anode and cathode is removed by conduction of the charge-carriers or magnetic J × B forces associated with the current flow. Removal of the plasma causes the switch to open. Pulse compressions to 50 nsec have been demonstrated on microsecond timescale charging.

5.2.2 Flux Compressors

A very different means of producing electrical pulses is the *magnetic flux compressor*, also termed the *explosive generator* and *magneto-culumative generator*.[6] The very high energy density of explosives, ~1 MJ/m^3 compared to capacitors at ~100 J/m^3, deforms conductors that enclose trapped magnetic flux. Flux conservation from an initial flux of I_0L_o gives a later current through the deformed inductor of

$$I(t) = I_0\, L_o/L(t) \tag{5.7}$$

And we can define a final current gain as $G_I = I_f/I_0$. But ideal flux conservation cannot hold true; there are ohmic losses and some flux escapes.[7] A figure-of-merit β for flux compressors is

$$G_I = I_f/I_0 = [L_o/L_f]^{\beta} \tag{5.8}$$

An ideal generator has $\beta = 1$, but typical values are $\beta \sim 0.6$ to 0.8 for the most widely used flux compressor, the helical generator shown in Figure 5.7. Note that the energy gain is

$$G_E = I_f/I_0 = [L_o/L_f]^{2\beta-1} \tag{5.9}$$

So no energy gain occurs for $\beta = 0.5$, though $G_I > 1$. To maximize both gains, L_o should by large, L_f small, and $\beta \sim 1$, or as close as possible.

The *helical generator* operates by a capacitor creating an initial current, therefore a flux in the *stator* winding. Detonation of the high explosive converts chemical energy into kinetic energy; flux compression converts it into electrical energy, a high current in the winding. The *armature* expands into a conical form and makes contact with the stator, shorting out turns in the winding as the point of contact progresses down the generator. The timescale for energy conversion is given roughly by generator length divided by the detonation velocity of the explosive, which is of the order 10 km/sec.

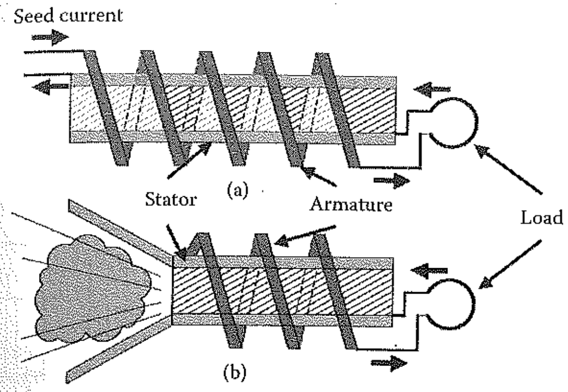

FIGURE 5.7
Helical flux compressor. Detonation of a high explosive converts chemical energy into kinetic energy; flux compression converts it into high current in the winding. Armature expands into a conical form and makes contact with the stator, shorting out turns in the winding as the point of contact progresses down the generator. (From Altgilbers, L., *Magnetocumulative Generators*, Springer-Verlag, New York, 2000. With permission.)

Figure 5.8 shows a helical generator driving a triode vircator with an inductive storage/opening switch pulse compression stage in-between. The current out of the generator (i_z) flows through the storage inductor and fuse, which explodes at peak current. The opening of the circuit creates an overvoltage on the spark gap, which closes, driving the anode to 600 kV positive voltage, and electrons are emitted into the vircator from the cathode (i_4). This all takes about 8 μsec, so microwaves are emitted from the horn before the shock wave from the explosion destroys the device. Microwave output is 200 MW in the S-band (~3 GHz).

Another microwave source that has been powered by flux compressor is the multiwave Cerenkov generator (MWCG; see Chapter 8). Here we see use of transformers, in part to get better rise times. Figure 5.9 shows the circuit: (1) a flux compressor (time-varying inductance and resistance) output is transformed up in voltage to charge an intermediate inductive store (2) with an opening switch (3), a fuse that explodes and produces ~1 MV into a pulse-sharpening output switch (4) into a diode (5), producing an electron beam into the Cerenkov generator. One clever feature is that some current from the transformer is diverted to drive the solenoid around the microwave source. The MWCG in Figure 5.10 produced microwaves similar in power and frequency to those of the above vircator. For a weapon concept that uses the flux compressor, see Section 3.2.2.

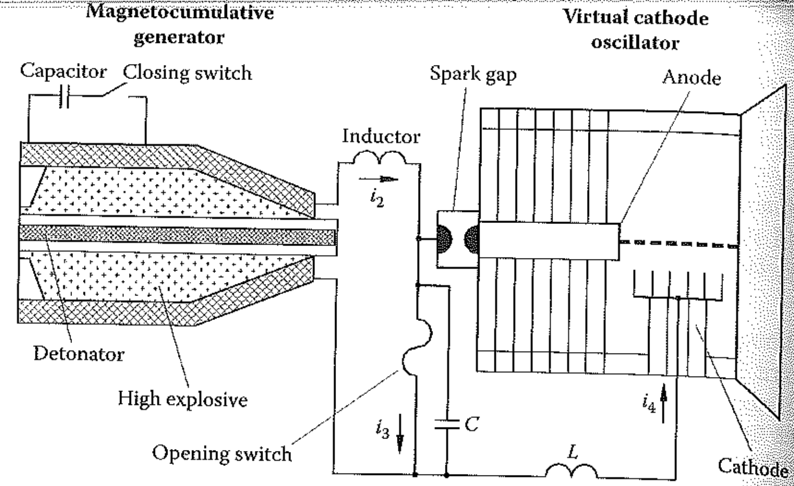

FIGURE 5.8
Helical generator driving a triode vircator through an inductive storage/opening switch pulse compression stage. Current out of the generator flows through the storage inductor and fuse, which explodes at peak current, opening the circuit, creating overvoltage on the spark gap that closes, driving the anode to 600 kV of positive voltage. The cathode emits electrons into the vircator; the microwave output is 200 MW in the S-band (~3 GHz). (From Altgilbers, L., *Magnetocumulative Generators*, Springer-Verlag, New York, 2000. With permission.)

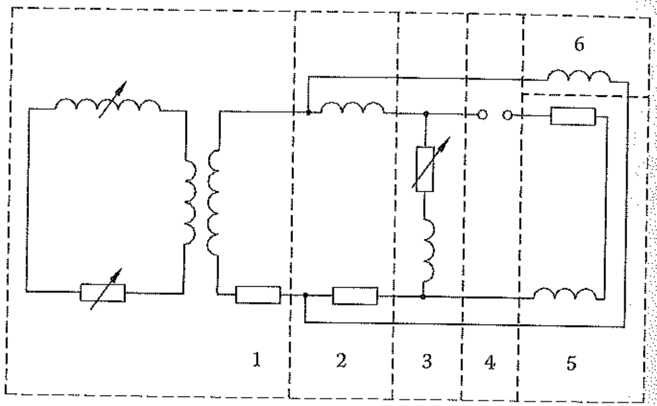

FIGURE 5.9
Circuit of driver for Figure 5.10: (1) flux compressor (time-varying inductance and resistance) output is transformed up in voltage to charge an intermediate inductive store (2) with an opening switch (3), a fuse that explodes and produces ~1 MV into a pulse-sharpening output switch (4) into a diode (5), producing an electron beam into the Cerenkov generator. Note some current from the transformer is diverted to drive the solenoid. (From Altgilbers, L., *Magnetocumulative Generators*, Springer-Verlag, New York, 2000. With permission.)

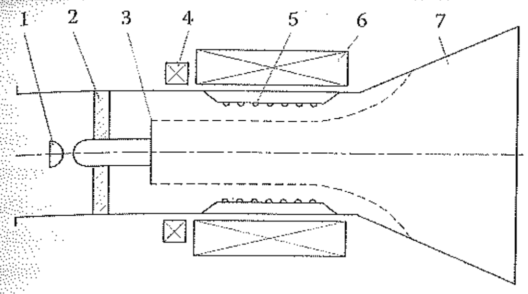

FIGURE 5.10
MWCG microwave source driven by circuit of Figure 5.9: (1) spark gap, (2) insulator, (3) cathode, (4 and 6) electromagnet, (5) slow-wave structure, and (7) antenna. (From Altgilbers, L., *Magnetocumulative Generators*, Springer-Verlag, New York, 2000. With permission.)

The *linear induction accelerator* (LIA) has been developed in the U.S. and U.S.S.R. over the last decade for particle accelerator and radiographic applications.[8] Its principal virtue is that the required accelerating voltage is distributed among a number N of pulse-forming subsystems so that full voltage appears only on the beam or a beam-emitting cathode (Figure 5.11). This technique, essentially a transformer distributed in vacuum, allows substantial downsizing of the pulsed power system. The LIA works as a series of 1:1 pulse transformers, each threaded by an electron beam or a solid cathode called a *voltage adder*. Each transformer section generates an increment of the voltage V on the cathode or beam, so that the peak voltage NV occurs at the

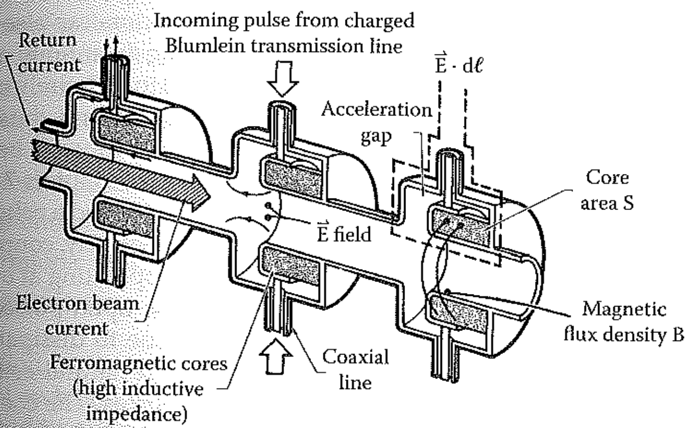

$$\oint \vec{E} \cdot d\vec{\ell} = -\int_S \frac{dB}{dt} \cdot d\vec{S}$$

FIGURE 5.11
Linear induction accelerator, an electron beam accelerated incrementally by induction cavities. Beam can be replaced by a solid cathode, which is then called a voltage adder.

tip of the cathode or in the exiting electron beam. The key component allowing summation of the voltage is a ferrite magnetic core in each of the accelerating cavities. These ferrite magnetic cores provide a high inductive impedance to a pulse arriving from a transmission line, so that the applied pulsed voltage appears as an electric field in the accelerating gap. The leakage current is small until the ferrite magnetic material saturates. At saturation, the cavity becomes a low inductance load and the pulse is shorted. Therefore, the core has a limit on the flux change that it can allow,

$$V\tau = A_c \Delta B \tag{5.10}$$

where τ is the pulse duration, A_c is the magnetic core cross-sectional area, and ΔB is the change of magnetic field in the core, which must be less than the saturation field of the magnetic material. LIAs are useful for short pulses of 100 nsec, but become very large and heavy for long pulses due to the magnetic core size.

A greater output voltage can be obtained by adding more cavities; the system is fundamentally modular. Moreover, because the pulsed power systems that drive the gaps operate at lower voltage, they are smaller and simpler to build. The drawbacks of the induction accelerator are that it is more expensive than pulse line technology for moderate voltages and that it is inefficient for low current. Because the pulse forming is conducted at lower voltage, the induction accelerator is appropriate for repetitive operation. The modular nature of the pulse-forming lines means that cooling of its N switches is easier than in a single accelerator stage, where energy is concentrated in a single output switch. Saturable inductors can also be used to perform several stages of pulse compression, giving an entirely magnetic system. The compression factor available per stage is 3 to 5. Entirely magnetic systems are attractive for long-life, repetitive operation, and thus will be used increasingly in HPM. Induction accelerators have thus far been used to drive free-electron lasers (FELs) and magnetrons (see Chapters 7 and 10). When the beam is replaced by a solid cathode, it is then called a *voltage adder*.

The requirement that HPM systems be operated repetitively, coupled with the desire for a compact, lightweight system, but still operating at both high peak and high average power, puts substantial stress upon pulsed power technologies. Operating repetitively, one has little time to dissipate excess energy due to source inefficiency; therefore, there is a natural coupling of repetitive operation with a preference for efficient sources. The cooling system required to handle dissipated power must be considered a fundamental element in a repetitive system; it may contribute a substantial weight, thus lowering the specific power of the system.

In summary, pulsed power systems used in HPM have been developed for other applications, but have served well. Pulse-forming lines are used for short (<200-nsec) pulse duration. Longer pulses require pulse-forming networks, which have yet to be extensively used in HPM. High-voltage transformers are used for repetitive operation because of their compactness and relative lack of complexity. LIAs (voltage adders or vacuum transformers) are more complex, while offering better average power handling. Magnetic energy storage is an emerging pulsed power technology that may have advantages in compactness, but operates at an impedance substantially lower than that of most loads. The primary challenge in pulsed power for HPM is repetitive operation, which remains relatively undeveloped.

5.3 Electron Beams and Layers

HPM sources tap the kinetic energy of electrons in a beam or layer to produce the intense microwave fields. To estimate the electron currents carried in these beams and layers, note that microwave power P is generated at some power efficiency η_p from an electron current I accelerated by a voltage V: $P = \eta_p VI$. The microwave power in pulsed sources is of the order of 1 to 10 GW, efficiencies are 10 to 50%, and voltages typically lie between several hundred kilovolts and several megavolts. Therefore, electron currents of 1 kA to several tens of kiloamps are typically required. In most cases, this current is carried by a beam of a specified cross-sectional profile at a high current density.

5.3.1 Cathode Materials

Production of an intense electron beam or layer begins at the electron source. The most common electron sources used in HPM devices are shown in Table 5.1 and are based on the following emitting phenomena[8] arranged in order of decreasing current density of emission:

- Explosive emission
- Field emission
- Thermionic emission
- Photoemission

In addition to the capacity for emitting at high current density, the attractiveness of each option depends on the requirements for quality of emission, as measured by spreads in the electron velocities and energies, ruggedness, and lifetime. No single source type is ideal for every application; the choice of technology is dependent on the HPM device in which it is to be used and the requirements of that device.

The most commonly used electron sources in present pulsed HPM devices are based on the process of *explosive emission*.[9] When low-impedance pulsed power applies high voltages to a metal cathode, average applied electric fields in excess of roughly 100 kV/cm at the emitting surface are further

TABLE 5.1

Cathode Materials for HPM

Emission Mechanism	Current Density	Current	Lifetime	Repetition Rate	Ancillary Equipment	Comments
Explosive						
Metal	~kA/cm^2	>10 kA	>10^4 shots	>1 kHz	Medium vacuum	Rapid gap closure
Velvet	~kA/cm^2	>10 kA	~10^3 shots	<10 Hz	Medium vacuum	Gas evolution limits repetition rate
Carbon fiber	~kA/cm^2	>10 kA	>10^4 shots	No limit	Medium vacuum	Rapid gap closure
CSi on C fiber	~30 A/cm^2	<1 kA	>10^4 shots	No limit	Medium vacuum	Slow gap closure
Thermionic	Arbitrary	~0.1 kA	>10^3 h	No limit	High vacuum; heater power	Heating to ~1000°C
Photoemission	ø	~0.1 kA	~100 h	No limit	High power laser; very high vacuum	

enhanced by the presence of naturally occurring micropoints.[10] The enhanced fields lead to the flow of large field emission currents through these micropoints, which rapidly heat and explode to form plasma flares within a few nanoseconds. Individual flares then expand and merge in 5 to 20 nsec to form a uniform electron emitter capable of providing current densities up to tens of kA/cm^2. The whole process, while destructive at the microscopic level, is not destructive of the emitting surface as a whole. The microscopic points are regenerated from one shot to the next, so that these sources can be reused many times. Explosive emission sources can be made from a wide variety of materials, including aluminum, graphite, and stainless steel. They produce the highest current densities of all options, are quite rugged, can tolerate poor vacuum conditions (the operationally limiting factor is arcing), and have reasonable lifetimes.

Principal research issues for explosive emission sources are:

- *Gap closure*: Ideally, the emission of electrons from the cathode is uniform and comes from a cool plasma with low closure speed. In reality, the plasma is often, as with a steel or graphite cathode, highly nonuniform with hot spots of rapidly moving plasma (called flares or jets), which rapidly close the diode gap and terminate microwave output. Such plasmas also make diode performance nonreproducible.
- *Uniformity*: Nonuniform or nonreproducible emission causes asymmetries that affect the ability of the beam to generate microwaves. Hot spots mentioned above result when only a few highly localized emission points carry the current. Therefore, solutions lie in producing more emission sites while not exacerbating the closure and outgassing issues.
- *Outgassing*: Outgassing of material during and after the pulse limits both the maximum attainable pulse repetition rate and the maximum burst duration for a given vacuum pumping speed. At any point during a burst, the diode current can be shorted out by an arc through the background neutral gas pressure that builds from pulse to pulse as the outgassed material is released.

To address these problems, use of fibers to produce uniform emission at lower electric fields began with carbon fiber cathodes.[11] Introduction of the CsI-coated cathode made major advances because CsI will light up more evenly due to its photoemissive properties: the copious UV light generated by electronic transitions in the cesium and iodine atoms/ions helps to encourage uniform emission. Many more points photoemit; thus, the current density is lower, ohmic heating is reduced, and the plasma is cooler. The surface then produces only heavy cesium and iodine ions with slow gap closure. Experiments have demonstrated reduction of closure velocity from 1 to 2 cm/µsec with bare carbon fiber to 0.5 cm/µsec when coated with CsI.

Nonexplosive field emission sources use macroscopic points or grooves on a surface to get enhanced electric fields. Arrays of tungsten needles, grooved graphite, and polymer–metallic matrices are examples of emitters of this type[12]; common velvet can also be a field emitter. Microcircuit fabrication techniques have been used to produce experimental arrays of metal-tipped emission points on a SiO_2 substrate.[13] Current densities ranging from several hundred A/cm^2 to several kA/cm^2 are achievable with field emission sources. Their advantages include the ability to operate at field levels below those required for explosive emission and, in this event, to avoid the creation of an expanding plasma at the emitting surface. A disadvantage of these sources relative to explosive emission sources is the lower peak current density achievable; source lifetime, particularly in the cloth emitters, is also a concern.

Thermionic emission is based on the heating of an emitting surface to allow electrons to overcome the work function and escape the surface.[14] No expanding surface plasma is required, and long-pulse to continuous electron beams can be produced. The most common thermionic emitter types are (1) pure materials such as tungsten and LaB_6, (2) oxide cathodes such as BaO, (3) dispenser cathodes, (4) cermet cathodes, and (5) thorium-based cathodes. Tungsten and thorium-based cathodes operate at temperatures too high to make them attractive. LaB_6 and the oxides produce current densities up to several tens of A/cm^2. LaB_6, however, must be polycrystalline at significant emitter sizes, which diminishes emission uniformity due to the differing current densities obtainable from the various crystal planes; further, at the high temperatures required for high-density emission (of the order of 2000 K), the chemical reactivity and mechanical stability of this material pose serious problems. Oxide emitters suffer from ohmic heating in the oxide layer at high current densities, as well as the problem of poisoning, a drastic reduction in emissivity with exposure to air or water vapor, from which they recover slowly and which requires high vacuum for their operation. Dispenser cathodes are used in the wide majority of conventional HPM tubes today. They consist of a porous plug of pressed and sintered tungsten impregnated with a mix of oxide materials. In the type B dispenser cathode, for example, the impregnant is a mixture of $BaO/CaO/Al_2O_3$ in the ratio 5:3:2, while the type M cathode is a dispenser cathode with the additional feature of having its surface coated with about 0.5 μm of a noble metal such as Os, Os-Ru, or Ir. A variant of the M-type dispenser cathode has produced current densities of almost 140 A/cm² at an operating temperature of about 1400 K in a vacuum of 10^{-7} torr. Cermet cathodes coated with a layer of Sc_2O_3, known as a scandate cathode, have emitted stable current densities of 100 A/cm² at 1225 K for thousands of hours in tests. Uniformity of emission, reproducibility, and a susceptibility to degradation by back ion bombardment are problems to be addressed for the scandates. Overall, the thermionic emitters have the advantage of being able to produce current densities up to the order of 100 A/cm² for long or continuous pulses. This current density is lower than those for the explosive and field emitters. Further disadvantages are the need for a cathode heater, which is usually large and heavy, and the tendency for poisoning at pressures above 10^{-7} or so.

In *photoemission* sources, the work function energy for electron emission from materials such as GaAs and Cs_3Sb is supplied by laser illumination.[15] These sources have the useful feature that electron emission can be turned on and off coincident with the laser pulse. Modulating the laser, therefore, has the effect of producing a beam that is effectively bunched. Further, because the electron emission is cold, with very little excess energy over that required for emission, random thermal motions of the electrons imparted in thermionic sources can be eliminated. Current densities as high as 100 to 200 A/cm² have been produced. The disadvantages of the photoemitters are the possibility of plasma formation at the surface if the laser intensity is sufficiently high, the complication of adding a laser to the system, and the requirement for vacuums as low as 10^{-10} torr.

The importance of emission quality varies with the type of microwave source. HPM sources with large Doppler upshifts in frequency, such as FELs and cyclotron autoresonant masers (CARMs), require very small spreads in the electron velocities and energies. Gyrotrons and backward wave oscillators (BWOs), for example, tend to be more tolerant of these spreads, and magnetrons and vircators are quite tolerant. In those HPM sources for which emission quality is important, quality is typically specified in terms of fractional velocity and energy spreads, or in terms of the *emittance* and *brightness*.[16] Here, we will define emittance as follows. Imagine that we cut a thin cross-sectional slice in the x-y plane from a group of electrons drifting in the z direction and measure the position and velocity of each electron in the slice. If we then plot the components of each electron in a two-dimensional phase space with axes for the x component of position and $\Theta_x = v_x/v_z$, the emittance ε_x is defined to be the phase space area filled by these points, divided by π; the units of ε_x are π•m•rad.* A similar definition applies for ε_y. After the electrons leave the source and are accelerated along z, the angle θ_x will decrease as v_z increases. It is therefore common to define a *normalized emittance* by, for example, $\varepsilon_{nx} = \beta\gamma\varepsilon_x$, where $\beta = v_z/c$ and $\gamma = (1 - \beta^2)^{-1/2}$. A third form of the emittance is the *root mean square (rms) emittance*, defined by $\varepsilon_{rms,x} = (\langle x^2\rangle\langle\theta^2_x\rangle - \langle x\theta_x\rangle^2)^{1/2}$; ε and ε_{rms} are proportional to one another, with a proportionality constant of the order unity, varying with the exact distribution of electron trajectories. It is important to note that emittance is a measure of both the size and collimation of a beam of electrons. A beam focused to a point might in fact have a relatively large emittance, because of the large value of θ required to bring the beam to a focus. On the other hand, a tightly collimated pencil beam would have a small emittance.

Brightness is defined at each point of a source or beam as the amount of current per unit area per unit solid angle. Rather than deal with this differential quantity, we will deal with the average edge brightness of a source or beam:

$$B = \frac{2I}{\pi^2 \varepsilon_x \varepsilon_y} \tag{5.11}$$

where I is the total emitted current; the factor π^2 takes account of the factor that appears in both ε_x and ε_y. As with emittance, we also define a normalized brightness, $B_n = B/(\beta\gamma)^2$. A plot of brightness for some different electron sources is shown in Figure 5.12.

5.3.2 Electron Beam Diodes

HPM sources employ electron beams generated from two-electrode diodes. The design of these accelerating structures to produce electron beams of high quality usually involves computer simulation to properly shape the electrodes and magnetic fields (if a field is used). Fundamentally, the basic features of diodes are illustrated by two idealized models, derived in Section 4.6.1:

- The *Child–Langmuir diode*, in practical units

$$J_{SCL}\left(\frac{kA}{cm^2}\right) = 2.33\frac{\left[V_0\left(MV\right)\right]^{3/2}}{\left[d\left(cm\right)\right]^2} \tag{5.12a}$$

* We display the factor π explicitly in the units for emittance because some authors define emittance without division by this factor.

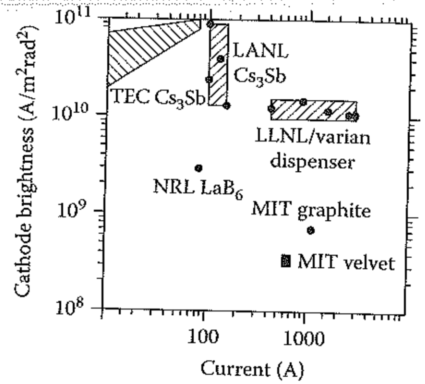

FIGURE 5.12
A comparison of cathode brightness vs. current for several different cathode emitters: field emission (velvet and graphite), thermionic emission (LaB_6 and a dispenser cathode), and photoemission (Cs_3Sb).

so with d ~ cm and the anode–cathode gap and ~1-MV potential applied from the pulsed power, current densities of kA/cm² and currents tens of kiloamps result. The current and impedance for a cylindrical cathode of radius r_c are

$$I_{SCL}(kA) = J_{SCL}A = 7.35\left[V_0(MV)\right]^{3/2}\left[\frac{r_c(cm)}{d(cm)}\right]^2 \tag{5.12b}$$

$$Z_{SCL}(\Omega) = \frac{136}{\sqrt{V_0(MV)}}\left[\frac{d}{r_c}\right]^2 \tag{5.12c}$$

Note that impedance is weakly dependent on the voltage, but very dependent on geometry.

- The critical beam current above which *beam pinching* occurs is estimated by equating the Larmor radius for an electron at the edge of the beam with the anode–cathode gap:

$$I_{pinch}(kA) = 8.5\frac{r_c}{d}\left[1+\left(\frac{V_0(MV)}{0.511}\right)\right] \tag{5.13}$$

Generally speaking, pinching complicates beam trajectories and is avoided in HPM sources (see Problem 2).

In all high power diodes there is the problem of *gap closure* due to the expansion of the cathode plasma. Gap closure has the effect of making the diode gap a time-dependent quantity: $d = d_0 - v_p t$, where closure velocities v_p are typically 1 to a few cm/μsec. Third, in order to extract the electron beam into a microwave source region, the anode must often be a screen or foil thin enough (i.e., much less than one electron range) that the electrons can pass through without undue angular scattering. The foil becomes a stress point in the design, since it will have a limited lifetime. Also, beam heating of the anode can create an anode plasma, which contributes to gap closure. Finally, the conducting anode will locally short the radial electric field of the beam, which disturbs the beam electron trajectories and introduces further spread in the transverse velocities of the electrons.

5.4 Microwave Pulse Compression

One way of generating high-peak microwave powers is to generate the microwaves in a long pulse at a lower power and then compress the pulse into a shorter duration at a higher peak power. The process can be seen as an extension of direct current (DC) pulse compression, i.e., pulsed power. Microwave pulse compression has been used for many years at low power levels for radar. At higher powers the problem of radio frequency (RF) breakdown limits the number of techniques that can be used. The contemporary work has been driven primarily by the need to obtain higher accelerating gradients in linear colliders, as described in Section 3.4. The practitioners of the art are now developing compressors in X-band and above for particle accelerators such as Compact Linear Collider (CLIC) and for studies of RF breakdown. Compressors have been studied as the basis of HPM weapons, compressing an accelerator-level klystron pulse (see Chapter 9) to ~50 nsec to reach >100 MW in a compact package. However, the Q requirements described below imply very narrowband components, so that such systems are very sensitive to frequency shifts.

The primary quantities of interest in pulse compression are, of course, power multiplication, pulse duration ratio, and overall efficiency. The standard definitions are:

$$M = \frac{P_1}{P_0}, \quad C = \frac{t_0}{t_1}, \quad \eta_c = \frac{M}{C} \tag{5.14}$$

where the initial pulse is characterized by P_0, t_0, and the final pulse is characterized by P_1, t_1. Compression efficiency η_c is generally high, and both M and C are of order 10 from most devices.

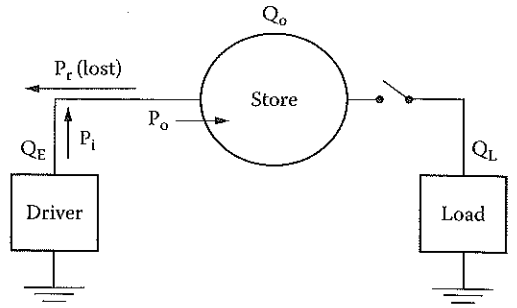

FIGURE 5.13
Microwave driver charges the store; switching into the load generates a high power, short microwave pulse. Q_E describes re-radiation of power back through the coupling port; Q_L is the extraction of stored energy.

The primary methods used for high power pulse compression are called switched energy storage (SES), SLAC (Stanford Linear Accelerator Center) Energy Development (SLED), and binary power multiplication (BPM). The most widely studied system is SES, which stores energy in a microwave store, then switches it to a load by a large change in the coupling to the load. Before describing specific devices, we first outline the general process of microwave pulse storage and compression.

Energy is stored in a high Q cavity and then released in a low Q external circuit. If a power P_o is injected into a storage cavity with quantity factor Q_o, the stored energy will approach $W_c \simeq P_oQ_o/\omega$. The cavity is then switched into a load for which the load quality factor is Q_L, much smaller than Q_o (Figure 5.13). The power extracted from the cavity will be

$$P_c = \frac{W_c\omega}{Q_L} = \frac{P_oQ_o}{Q_L} \tag{5.15}$$

The power multiplication is

$$M = \frac{P_c}{P_o} = \frac{Q_o}{Q_L} \tag{5.16}$$

If there were no losses, energy would be conserved and power out would increase linearly with the Q-switching ratio, but losses always reduce performance below the above. Storage resonators made of copper have internal Q factors of 10^3 to 10^5. For superconducting resonators, Q values of about 10^9 can be achieved. However, the power multiplication and pulse compression that can be obtained in practice depend upon several other technological factors. Copper cavities are frequently limited by the rise time of the switch element because losses occur during switching. For superconducting cavities, a major limitation is the requirement of very high stability in the resonant frequency of the store and the frequency of the oscillator charging the store. Energy will be reflected from the store if the incoming pulse differs from the resonant frequency of the store. Efficient accumulation of energy in superconducting devices requires extraordinary stability of these two frequencies, of the order $Q_o^{-1} \sim 10^{-9}$.

Some of the injected energy will be reflected from the input port to the store. The external quality factor Q_E describes the re-radiation of power back through the coupling port and is determined by geometry of the port and its field structure. The coupling parameter β is

$$\beta = \frac{Q_o}{Q_E} \tag{5.17}$$

In a steady state the ratio of reflected–to–incident power is

$$\frac{P_r}{P_i} = \frac{(1-\beta)^2}{(1+\beta)^2} \tag{5.18}$$

Therefore if $Q_o = Q_E$, $\beta = 1$ (critical coupling), there is no reflected power. Power is reflected in either the undercoupled ($\beta < 1$) or overcoupled ($\beta > 1$) case. Then the stored energy is reduced and the power released is

$$P_c = 4P_o\left(\frac{\beta}{1+\beta}\right)^2 \tag{5.19}$$

and power multiplication is

$$M = \frac{P_c}{P_o} = \frac{4Q_E}{Q_L}\left[\frac{Q_o}{Q_o+Q_E}\right]^2 \tag{5.20}$$

For good pulse compression, the ordering of Q values is $Q_o >> Q_E > Q_L$. Since energy is lost to heating the walls, optimization depends on the time taken to fill the store. As an example, consider an S-band conventional klystron charging a copper store cooled to liquid nitrogen temperature. The rectangular waveguide cavity has $Q_o = 4.5 \times 10^4$, so $Q_o/\omega \sim 2.4$ μsec. With a coupling factor $\beta = 3.5$, the 10-MW klystron injects 20 J in 2 μsec, of which 12 J is stored for an efficiency of 60%.

The switched energy storage device most widely studied is shown in Figure 5.14. Energy is slowly stored in the cavity so that RF fields are high. The output branch is an H-plane tee located $\lambda/2$ from the end wall. Therefore, there is a voltage null on the output side branch leading to the load, and little coupling

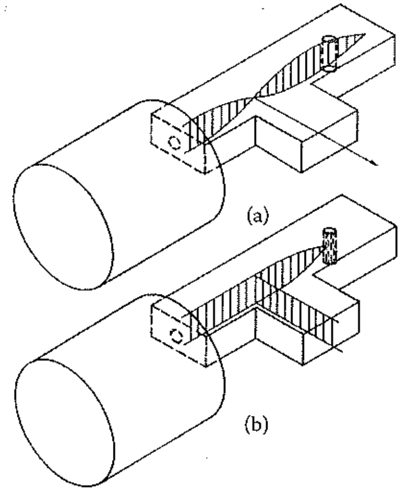

FIGURE 5.14
Switched energy storage system: microwave store and H-plane tee showing electric field envelope in (a) storage state and (b) dump state.

occurs between the cavity and the load. The triggering event is the creation of electrically conducting plasma at $\lambda/4$ from the shorted end of the waveguide, creating a tee null at the switch point and a field maximum at the output aperture. Energy from the cavity then dumps into the load on a short timescale.

The *dump time* from a store depends on the volume, V, of the cavity, the total area, A, of the output ports, and the group velocity, v_g, in the output waveguide. The dump time is crucially dependent upon the geometry of the cavity mode in the store and the precise location of the port in relation to the field geometry. An estimate of the dump time is[17]

$$t_D \equiv t_1 \approx \frac{3V}{Av_g}\left|\frac{B_P}{B_o}\right|^2 \qquad (5.21)$$

where B_p is the RF magnetic field at the port and B_o is the maximum magnetic field in the cavity. For example, a spherical cavity of 20 cm radius with four output ports, each with a 15-cm^2 area, gives a dump time of ~100 nsec, about that needed for RF accelerators.

The cavities store an energy density of ~1 kJ/m^3 at electric fields on the order of 100 kV/cm. The switch is the crucial element in this scheme and must support such fields while open during storage time, but switch quickly with low loss when closed at the desired release time. Several switching mechanisms have been studied: spontaneous breakdown of a gas in the waveguide, high-voltage plasma discharge, vacuum arc, and an injected electron beam. The most widely used switch is the plasma discharge tube (triggered or self-breaking, with the former giving better performance).

The original experiments by Birx and coworkers[18] used a superconducting cavity with $Q_o \simeq 10^5$ and $Q_L \simeq 10^4$, so $M \simeq 10$. The Tomsk group used a 3.6-µsec, 1.6-MW S-band klystron. At extraction, pulse durations from 15 to 50 nsec were obtained at powers to 70 MW, giving M ~ 40, C ~ 200.[19] Extraction efficiency from the resonator is reported as 84%; overall conversion efficiency is about 30%. Alvarez and coworkers[20] report 200-MW, 5-nsec pulses from a 1-µsec, 1-MW drive, so that M ~ C ~ 200. However, overall efficiency is reported to be 25%. Detailed work by Bolton and Alvarez has reduced the prepulse in the SES pulse compression scheme. Typically, a prepulse occurs at –40 dB below the main pulse. In their balancing scheme, the decoupling between the resonator and the load was reduced to –70 dB. The Tomsk group[21] used an S-band vircator at 400 MW injected into an SES. Because of the broadband nature of the vircator and the narrow bandwidth of the SES, only 20 MW of the 550-nsec pulse was accepted. The compressed pulse was 11 nsec at 350 MW, giving M = 17.5, C = 45, and η_c = 38%.

We now consider storage systems in which the switching is performed by phase reversal. In the SLED method of pulse compression, two high Q cavities store energy from a klystron. Release of the energy from the store is triggered by a reversal in the phase of the klystron pulse. Switching takes place at low power levels at the amplifier input. Farkas et al.[22] gives an analysis of the energy gain of a SLED system. The maximum obtainable is M = 9. However, the shape of the output pulse from SLED is a sharply decaying exponential, which makes the effective power gain substantially less than the theoretical value. SLAC is now operating with 60-MW, 3.5-µsec klystron pulses compressed in SLED to 160 MW, 0.82 µs, giving M = 2.67, C = 4.27, and an overall compression efficiency of 62%. This attractive efficiency coupled with the relatively simple construction is why the method is currently used worldwide in many electron accelerators.

Because of the limited power gain of SLED, another form that gives a flat output pulse was developed, called the Resonant Line SLED (RELS; also called SLED II). The resonant line shown in Figure 5.15 is simply a transmission line coupled to a source through a network and terminated in a short. The distance between the network and the short must be a multiple of half-guide wavelengths. The final output pulse duration is the round-trip delay between the network and the short. The line is charged and the phase of the input signal is reversed, causing a discharge of the resonant line. In effect, this is very much like the transient charging of a pulse-forming line as described in Section 5.2, except the charging energy is microwave, not DC. Figure 5.16 shows the output field and output power in terms of the round-trip delay time, T_r. The dashed line shows the reversal of phase that triggers the output pulse. Calculations predict that the power gain and compression factors are typically 4, with a compression efficiency of about 80%.

Dissipation loss is minimized by using storage elements consisting of overmoded TE_{01} circular guides. For this mode, loss decreases as the cube of the diameter at fixed frequency. It is possible to stage RELS, limited by line attenuation losses and coupling mismatches. Thus far, a single RELS has been dem-

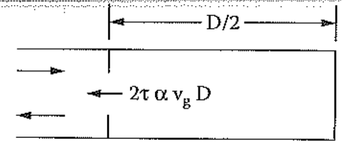

FIGURE 5.15
Schematic of resonant line storage system.

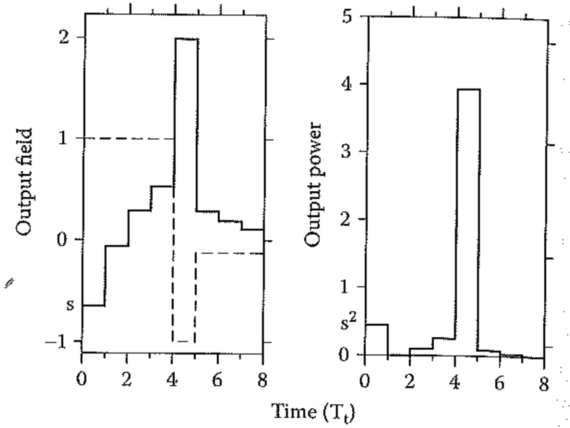

FIGURE 5.16
RELS single-stage output field and output power vs. time in units of T_f. Dashed line shows input phase modulation.

onstrated experimentally at quite low powers. A high power RELS system with a goal of 500 MW was under development at SLAC. Calculations show that for two-stage RELS, power gain could be 10 with an efficiency of about 60%.

The *binary power compressor* (BPC) is a device that multiplies microwave power in binary steps. Each step doubles the input power and halves the pulse length. Compressors of up to three stages have been operated at efficiencies of 45%. The BPC produces a rectangular output pulse. As with RELS, dissipation is reduced with the use of overmoded waveguides. This is an important feature for BPC because waveguides are quite long. As with SLED, the active control element operates only at low power. Passive elements (delay lines and 3-dB couplers) operate at high power. Couplers have been operated at SLAC at power levels in excess of 100 MW.

5.5 Antennas and Propagation

At the interface between the HPM source and free space, the two features of HPM that stress conventional antenna technology are high power and short pulse duration. Consequently, HPM antennas have been direct extrapolations of conventional antenna technology, usually in simple form, with allowance made for high electric field effects and for the shortness of the pulse.

5.5.1 Mode Converters

Between generation and radiation of microwaves, there is an opportunity to convert from one waveguide mode to another. *Mode conversion* goes back to the earliest days of microwaves, when it was called *mode transformation*.[23] This usually means:

- Converting from TE to other TE modes or from TE to TM (because TM, the right mode for interacting with the E_z component of modulations on the electron beam, has an unfortunate null on axis when radiated)
- Converting from circular to rectangular waveguide (so as to connect to antenna hardware)
- Converting directly from a waveguide mode to a radiating mode

The early method was to simply project an electrode from one waveguide into another. For example, the center electrode of a coaxial cable would be inserted into the center of a rectangular waveguide parallel to the short dimension. Such methods can be made efficient, but abrupt transitions will break down at high powers.

To finesse high power breakdown, slow transitions are the method. For example, the TM mode output of the relativistic klystron in Figure 9.20 is converted into the useful rectangular TE_{01} mode using the method shown in Figure 9.26. Radial fins are slowly introduced into the center conductor of the coax at the output end and grow until they reach the outer conductor, where they divide and adiabatically transform into a rectangular cross section. Such a converter has been built for a high-current S-band klystron and has been operated at 20 MW, although it suffered from breakdown due to too-short transition sections.

In gyrotrons, the rotating electrons interact with high-order cavity modes in the millimeter regime.[24] The high frequencies require *quasi-optical* mode converters. They use geometrical optics to ray-trace TM and TE modes, which are essentially decomposed into plane waves, each propagating at angles to the waveguide axis and each undergoing successive reflections from walls and mirrors. Such methods are used extensively for gyrotrons in fusion heating to provide transport of microwaves over long distances with little loss (see Chapters 3 and 10).

Direct conversion from waveguide to radiating waves is exemplified by the Vlasov convertor,[25] shown in Figure 5.23a. The TE mode k-vectors are reflected from a curved conductor and, if dimensions are chosen correctly, produce a Gaussian-shaped beam at an angle to the waveguide axis. For TM converted directly into a Gaussian beam.

5.5.2 Antenna Basics

The *directive gain* of an antenna is its ability to concentrate radiated power in a particular direction. It can be expressed as the ratio of beam area Ω_A to the 4π steradians of all space:

$$G_D = \frac{4\pi}{\Omega_A} = \frac{4\pi}{\Delta\theta\Delta\Phi} \tag{5.22}$$

where the beam widths in the two transverse dimensions are $\Delta\theta$ and $\Delta\phi$. Directivity is frequently defined as the ratio of the power density S in the main beam at a distance R to the power density from an isotopic source radiating total power P:

$$G_D = \frac{4\pi R^2}{P} S \tag{5.23}$$

The *gain*, G, is G_D times the antenna efficiency:

$$G = G_D = \frac{4\pi A\varepsilon}{\lambda^2} \tag{5.24}$$

A is the antenna physical area, or radiating *aperture*, and ε the design-dependent antenna efficiency, due to power fed to the antenna but lost so not radiated, typically 0.5 to 0.8. Here we have introduced directivity in terms of antenna area. The product GP is the *effective radiated power* (ERP). Figure 5.17 graphs power densities for typical HPM cases (see also the nomograph; Figure 3.9). Note that the common way to describe gain is in decibels, G_{dB}. This value corresponds to an actual numerical value of

$$G = 10^{G_{dB}/10} \tag{5.25}$$

so a gain of 100 is called 20 dB (see Problem 3).

The radiation field of an antenna is not a simple spotlight, but has several regions. Moving away from the aperture, the regions are:

- *Reactive near-field region*, where the electromagnetic fields are not yet fully detached from the launching antenna and reactive terms dominate.

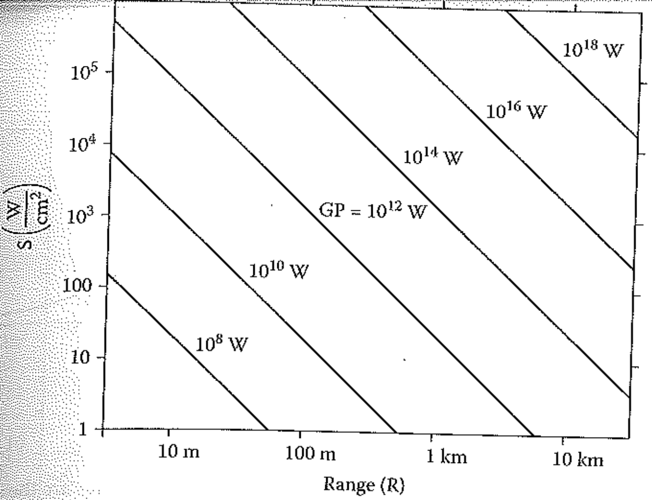

FIGURE 5.17
Power density at range for various effective radiated powers.

- *Radiating near-field region* (also *Fresnel region*) beginning at $0.62\sqrt{\frac{D^3}{\lambda}}$, where D is the antenna diameter. Radiation fields dominate, but angular field distribution depends on distance from the antenna. The beam is roughly cylindrical with varying diameter and intensity, reaching a peak at about $0.2\ D^2/\lambda$. From this point, the intensity drops monotonically, approaching $1/R^2$ falloff.
- *Radiating far-field region*, where the wave is truly launched, arbitrarily defined as the location at which the phase wave front differs from that of the circular by 5% of a radian:

$$L_{ff} = \frac{2D^2}{\lambda} \tag{5.26}$$

For example, consider the field of a horn antenna, shown in Figure 5.18. Its general features are the same for most antenna types.

The degree of phase uniformity that is acceptable for a test is an important question because it sizes the anechoic room used for testing and limits the power density available from a specific source. Points beyond $0.2L_{ff}$ are used for HPM vulnerability testing. L_{ff} can be located within a specific room by using a lower-gain antenna (smaller antenna or lower frequency), as long as air breakdown is avoided.

One of the most important aspects of antennas is their sidelobes, which are produced by diffraction from edges and feeds. Figure 5.19 shows that the

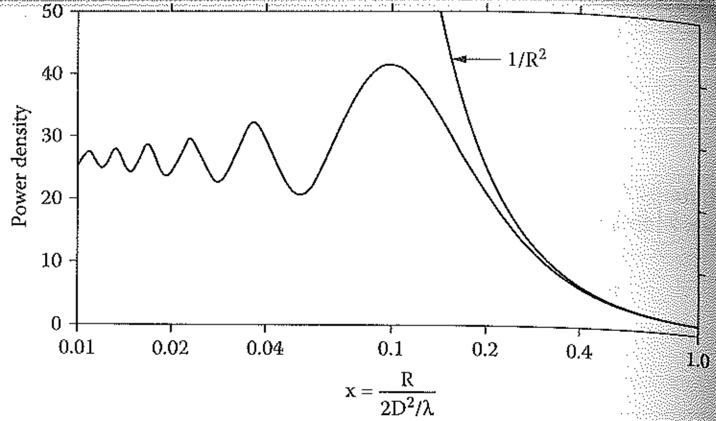

FIGURE 5.18
Horn antenna intensity normalized to unity at $2D^2/\lambda$. Its general features are the same for most antenna types.

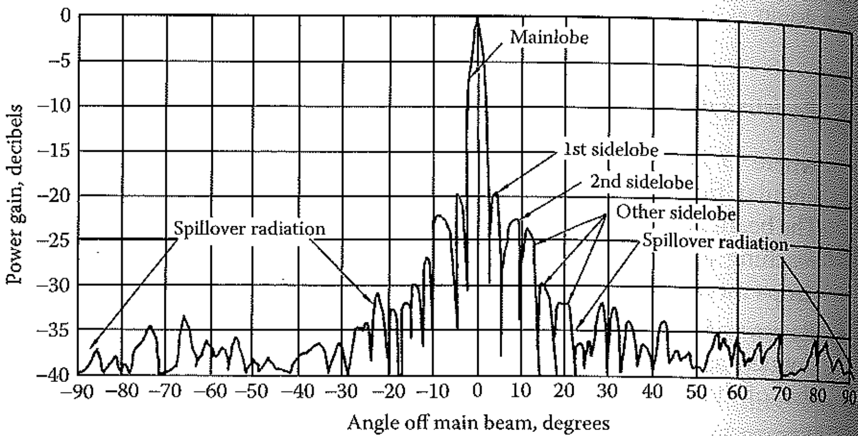

FIGURE 5.19
Example of radiation pattern at high angles to beam.

main lobes are accompanied by lobes at higher angles from diffraction at the antenna edge. There is also a backlobe at 180° to the main beam. In the far field, these effects are small indeed, but near the antenna the fluences can be very large. These elements of the radiation pattern cause concern over potential damage to nearby electronics (fratricide and suicide; see Section 3.2.1).

Once launched into the air, the key issue in HPM antenna design is breakdown. This occurs when the local electric field is sufficient to accelerate an electron to energy high enough to collisionally ionize gas atoms or to cause flashover at the air–waveguide interface. A cascade breakdown ensues, forming a conducting region from which the electromagnetic wave can be reflected or absorbed. The crucial factor is that the electron ionization rate

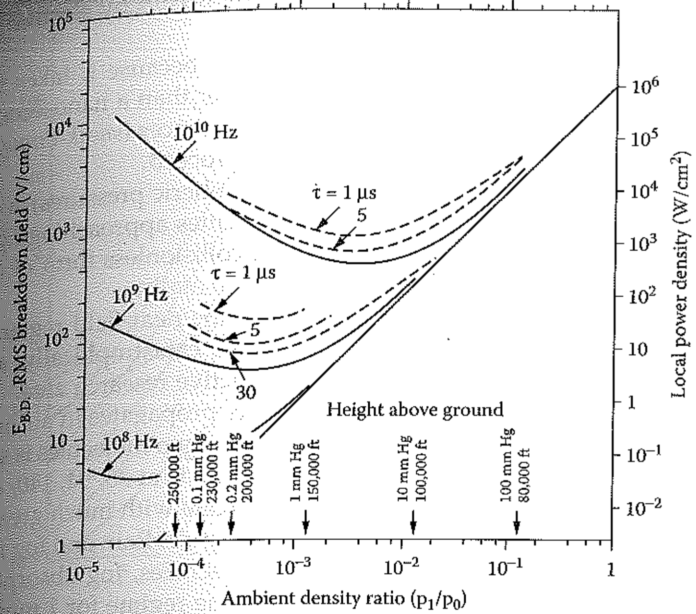

FIGURE 5.20
Microwave breakdown of ambient air at various altitudes, pulse durations, and frequencies.

exceeds the rate electrons are attached to ions. At high pressures, the critical fluence for air breakdown for pulses longer than a microsecond is

$$S\left[\frac{MW}{cm^2}\right] = 1.5\rho^2(\text{atm}) \tag{5.27}$$

where p is the pressure in units of an atmosphere. This corresponds to a critical field of 24 kV/cm at atmospheric pressure. At high altitudes, only low power densities can propagate. The minimum point is at between 20 and 50 km, depending on frequency (see Figure 3.25). Breakdown thresholds are high at high pressure (because there are many collisions) and at low pressure (because there is no cascade). Lowering the pressure will allow breakdown at lower fluences, as shown in Figure 5.20 [useful formula: $E(V/cm) = 19.4\,[S(W/cm^2)]^{1/2}$]. The pressure dependence of breakdown is of particular importance for HPM applications that involve radiation from aircraft at high altitudes or from sources beaming either upward from the ground or downward from orbit.

A crucial region is at ~50 km altitude, where a microwave pulse experiences gradual energy loss due to *tail erosion*. The head of the pulse continually ionizes the atmosphere, creating an absorptive plasma through which the tail must propagate. At 50 km, the threshold is about 250 W/cm².[26] For pulses of 100 nsec, a plasma *ionospheric mirror* can form at 50 km that reflects microwaves at low frequencies (~1 GHz) and dissipates by electron attachment and recombination in many milliseconds.

Breakdown is dependent upon pulse duration because it takes time to develop, leading to speculation that pulses shorter than a nanosecond may propagate through the atmosphere at very high fluences (*sneak-through*), i.e., insufficient time is available for breakdown to proceed.

At very high fluences (~10^3 MW/cm^2 at atmospheric pressures), a relativistic regime occurs when electrons achieve velocities approaching light and pondermotive forces come into play, giving a collisionless form of absorption. This regime has not been explored experimentally.

When breakdown occurs, hot spots occur in the near-field region of the antenna, causing reflection of waves, gain falls catastrophically, and the breakdown region spreads. This process is an active research area.

Once launched, the microwave pulse typically propagates in air modified by weather. Absorption in the air by water and oxygen molecules is strongly frequency dependent (Figure 5.21), giving passbands at 35, 94, 140, and 220 GHz. Lower-frequency pulses (<10 GHz) propagate with much greater efficiency over extended distances than the higher bands. Rain and fog increase microwave absorption. At low-microwave frequencies, fog absorptivity is 0.01 to 0.1 dB/km; rain absorptivity is in the same regime for 1 mm/h rain (see Problems 4 and 5).

5.5.3 Narrowband Antennas

Antennas for HPM narrowband have mostly been straightforward extrapolations of conventional antenna types modified to prevent air breakdown. Antenna arrays are just coming into development, principally for use in phase-locked multiple oscillator or amplifier systems. High power antenna subelements, such as phase shifters and splitters, have received little attention to date.

In practice, only a few types of antennas have been used in narrowband HPM. The gains of the principal types are shown in Table 5.2.[27] The most common type is the horn — pyramidal, conical, and transverse electromagnetic (TEM). Its utility follows from its similarity to a waveguide; horns are usually constructed as a flare from a rectangular or circular waveguide extending directly from the source. Conversion to a useful mode is a key issue in all applications. Generally, the fundamental modes (TE_{10} in rectangular guide, TE_{11} in circular) are preferred in part because they radiate onto useful patterns. As long as air breakdown is avoided by having an aperture large enough to reduce the electric fields when the wave enters air, the radiation pattern of horn antennas can be exactly calculated from first principles. Figure 5.22 shows the radiation pattern measured by Sze et al. from a TE_{10} rectangular horn at 2.8 GHz.[28] The pattern is linearly polarized with gradual falloff, making it useful for electronic vulnerability testing (as opposed to TM_{on} patterns, which are polarized with a radial electric field and have a highly nonuniform donut pattern).

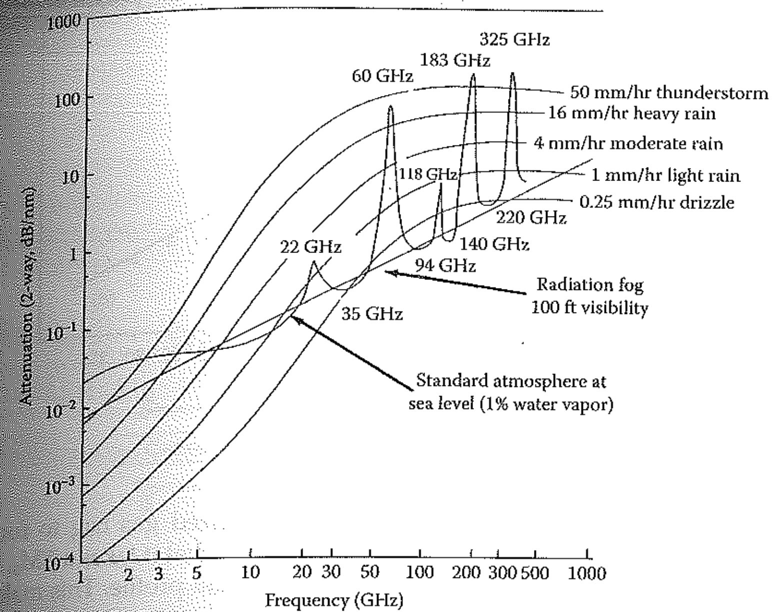

FIGURE 5.21
Atmospheric and rain attenuation for two-way propagation (as in radar). Note vertical scale is for 2-way transmission, as for radar, and nm = nautical mile.

TABLE 5.2
Principal Antenna Types

Antenna	Gain	Comments
Pyramidal and TEM horn	$2\pi ab/\lambda^2$	For standard gain horn; sides a, b; lengths $l_e = b^2/2\lambda$, $l_h = a^2/3\lambda$
Conical horn	$5\,D^2/\lambda^2$	$l = D^2/3\lambda$; D = diameter
Parabolic dish	$5.18\,D^2/\lambda^2$	
Vlasov	$6.36\,[D^2/\lambda^2]/\cos\theta$	Angle of slant-cut θ, $30 < \theta < 60$
Biconic	$120\,[\cot \alpha/4]$	α is the bicone opening angle
Helical	$[148\,N\,S/\lambda]\,D^2/\lambda^2$	N = number of turns; S = spacing between turns
Array of horns	$9.4\,AB/\lambda^2$	A, B are sides of the array

Parabolic dish antennas are ubiquitous in conventional microwave applications, but have found little use in narrowband HPM because the centralized feed of the parabolic antenna contains very high fields. However, in ultrawideband, a dish antenna called the Impulse Radiating Antenna (IRA; see Section 6.3) is the leading type. A variant is the Flat Parabolic Surface (FLAPS) antenna discussed in Section 3.2.3.

The Vlasov antenna[29] is well suited to launch narrowband HPM radiation. It has a simple construction with a relatively large feed aperture that helps to suppress or avoid RF breakdown. If its primary aperture is too small to support the microwave fields that it is attempting to launch, it can be easily